DPSP 56-25-80



This document consists of
34 pages, No. 2 of
30 copies, Series A .

# FUEL TEMPERATURE COEFFICIENT OF REACTIVITY

° ° ° ° ° ° ° ° ° ° ° ° ° ° ° ° ° ° °

W. E. Loewe

November 30, 1956

RESTRICTED DATA



E. I. du Pont de Nemours and Company
Explosives Department - Atomic Energy Division
Savannah River Plant

This document was prepared in conjunction with work accomplished under Contract No. AT(07-2)-1 with the U.S. Department of Energy.

## DISCLAIMER

[redacted]

## Distribution

### Wilmington

1 J. E. Cole
2 H. Worthington
3 D. F. Babcock
4 R. L. Menegus
5 J. B. Tinker
6 H. W. Bellas
7 M. H. Smith
8 W File

### Savannah River Plant

9 D. A. Miller
10 J. A. Monier
11 F. H. Endorf
12 M. H. Wahl
13 G. Dessauer
14 D. S. St. John
15 J. L. Crandall
16 H. D. Brown
17 W. P. Overbeck
18 A. A. Johnson
19 F. E. Kruesi
20 P. A. Dahlen
21 L. W. Fox
22 E. W. Hones
23 W. E. Loewe
25 TIS File
26 TPO File
27-29 PRD Extra Copies
30 PRD Record Copy

### Atomic Energy Commission

24 H. L. Kilburn, SROO



[redacted]

## Contents



## Abstract


A method for measuring the fuel temperature coefficient of reactivity in a heterogeneous nuclear reactor is presented. The method, which is used during normal operation, requires that calibrated control rods be oscillated in a special way at a high reactor power level. The value of the fuel temperature coefficient of reactivity is found from the measured flux responses to these oscillations.

Application of the method in a Savannah River reactor charged with natural uranium is discussed.

## Introduction

Important features in the design and operation of a nuclear reactor are the ease with which the reactor can be controlled and those characteristics of its kinetic behavior which contribute to safe operation. A strong factor in a reactor's stability is the amount by which the reactivity changes in response to a temperature change in the system.

In a heterogeneous reactor, the fuel temperature coefficient of reactivity (represented by the symbol $\Lambda$ ) is especially significant because of the rapidity with which the fuel temperature can change after a change in reactor power level. Therefore, the sign and magnitude of $\Lambda$ are important considerations in design and operation.

It is difficult to calculate the magnitude of $\Lambda$, and in some cases the sign of $\Lambda$ may be in doubt. Thus, there is a need for an experimental technique by which $\Lambda$ may be measured. Such methods usually require special equipment or lattice modifications which change the known characteristics of the reactor and usually interrupt normal reactor operation. Most experimental methods also require extrapolation from measurements on small samples to obtain a value of $\Lambda$ in a full reactor charge. An experimental technique for measuring $\Lambda$ which does not suffer from these disadvantages was sought.

## Summary

A method has been developed to measure $\Lambda$ in a nuclear reactor. It consists of three main steps:

1. At a normal operating reactor power level, calibrate a group of control rods by a special oscillation technique.

2. At the same power level, oscillate the calibrated control rods on a cycle of motion specially chosen for the sensitivity to fuel temperature changes of the thermal neutron flux response.

3. Adjust the value of $\Lambda$ in a calculation of the neutron flux response to these oscillations so that the measured and calculated responses agree.

Steps 1 and 2 may also be performed at a very low reactor power level to test the validity of the calculations in the special case where temperature effects are negligible.

This technique has the advantages listed on the following page.

- Measurements are made during normal reactor operation.
- Measurement can be made in a short time. This feature makes feasible a study of the dependence of $\Lambda$ on reactor conditions (eg, fuel exposure).
- No auxiliary equipment is required.
- The reactor is unchanged by the measurement, and no extrapolation from a small sample is necessary. The technique provides a value of $\Lambda$ for the full complement of fuel elements in their normal configuration.

The method gave a value of $-1.3 \times 10^{-5}$ $\Delta k/°C$ for $\Lambda$ in a Savannah River reactor containing a full charge of natural uranium (Mark I) fuel elements.

## Discussion

The method described here for measuring $\Lambda$ was first used in a Savannah River reactor containing a natural uranium (Mark I[1]) charge. Although its applicability is not limited to that type of reactor, clarity in exposition will be promoted in this report by restricting the discussion to this particular application.

A Savannah River reactor containing a natural uranium (Mark I) fuel charge is described briefly in appendix A. Also described is the differential electrometer, the instrument used for measuring thermal neutron flux oscillations, which is characterized by variable sensitivity, short time constant, and provision for subtraction of a constant component from an oscillatory signal.

Appendix B presents reference information for understanding the response of the reactor to oscillations of a neutron absorber within the reactor. The technique for calibrating control rods by oscillating them in a sawtooth pattern, called the "oscillation technique" in this report, is also described briefly.

### Objective

Measurement of $\Lambda$ requires three essential steps performed at normal reactor operating power level. (The higher the power level at which the measurements are made, the higher the fuel temperatures and the greater the precision in the measurement of $\Lambda$.)

[1] See appendix A for description of a Mark I fuel element.

These steps are:

1. Calibrate a group of control rods.

2. Oscillate these control rods on a truncated sawtooth cycle, and measure the neutron flux response.

3. Find $\Lambda$ from the data obtained in steps 1 and 2. The effective $\Lambda$ is that value which, when used in reactor kinetics calculations, produces agreement between the measured and calculated flux response to the oscillations performed in step 2.

## Experimental Procedure

Control Rod Strength. Control rod gangs (see appendix A) are calibrated to within ± 10% by oscillating them on an 8-second sawtooth cycle (see appendix B, page 27). This calibration, which yields $\Delta k_{eff}$/cm over a 12-cm interval, is performed at the normal reactor operating power level with whatever control rod configuration obtains at the time.

During the (truncated sawtooth) control rod oscillations discussed below, the extreme positions of the control rods are recorded from a meter on the reactor operating console. This information, plus the $\Delta k_{eff}$/cm for the control rods obtained from the 8-second sawtooth oscillation, provides the total $\Delta k_{eff}$ caused directly by the motion of the control rods, with a precision of ± 10%.

Truncated Sawtooth Oscillations. The calibrated control rods are oscillated on the truncated sawtooth cycle shown in figure 1 for $\Sigma_a$, the effective macroscopic absorption cross-section for thermal neutrons. Figure 1 also shows $k_{excess}$, and the fluxes near and far from the oscillated rods, when $\Sigma_a$ has a truncated sawtooth variation. The change in flux during the motionless part of the control rod ($\Sigma_a$) cycle is referred to as the "period" rise or fall.

Cycles of several different lengths are used to display the variation of flux response with cycle length. A minimum of one second is set for each distinct part of the oscillation cycle by the practical limitation of manual operation of the remotely controlled rods. The movement of the control rods from their equilibrium position is limited to a maximum time interval of two seconds to avoid flux changes of sufficient magnitude to cause thermal strains in the reactor structure. (Larger intervals offer no advantages, since a sufficiently large $\Delta k_{eff}$ is introduced in two seconds.) The length of the motionless part of the rod cycle, corresponding to the "period" part of the flux rise, is restricted to ten seconds to prevent the moderator temperature from changing substantially (see appendix B).

Examples of the flux response to control rod oscillations of this type are shown in figures 2 and 3. These are traces obtained from the differential electrometer. Figure 2 shows the response obtained in a reactor operating at a very low power (ca 1 mw); and figure 3 shows the response at 450 mw.

The amplitude of the "period" part of the flux response, divided by the equilibrium flux level, is defined as $\Delta\Phi^*_{100}$. The symbol refers to both the positive and negative halves of the oscillation cycles, which are the same after initial transients have died out (after about $1\frac{1}{2}$ cycles). Thus for a typical set of ten cycles, seventeen separate measurements of $\Delta\Phi^*_{100}$ are made, and a good average value can be obtained. However, it is better to use $\Delta\Phi^*_{75}$, defined as the relative flux change between an extreme and the point preceding in time by 75% of the length of the "period" part of the oscillation cycle. This allows more satisfactory processing of data, since it eliminates finding the exact point on the flux response trace where the "period" part begins. (Since the flux varies rapidly here, an error in determining this point introduces more error in $\Delta\Phi^*$ than a similar error at 75%.) Figure 4 makes the measurement clear. For convenience, the subscript 75 will be dropped henceforth, and $\Delta\Phi^*$ will be understood to be $\Delta\Phi^*_{75}$.

$\Delta\Phi^*$ is independent of the position at which it is measured, and is that part of the flux response which is sensitive to pile reactivity changes caused by changes in the temperatures of reactor components (see appendix B). The quantity $\Delta\Phi^*/\Delta k$ can then be obtained from the measured values of $\Delta\Phi^*$ and $\Delta k$ for each type of cycle. $\Delta\Phi^*/\Delta k$ is independent of $\Delta k$ over a wide range, and is therefore a convenient quantity for comparisons.

Values of $\Delta\Phi^*/\Delta k$ which have been obtained are shown in tables 1 and 2. Table 1 shows $\Delta\Phi^*/\Delta k$ measured in a reactor operating at about 1 mw (average fuel temperature ca 8°C); and table 2 shows $\Delta\Phi^*/\Delta k$ at 450 mw (average fuel temperature ca 170°C). The differences between the values shown in tables 1 and 2 are an indication of the sensitivity of $\Delta\Phi^*/\Delta k$ to temperature-induced reactivity changes.

In order to display this sensitivity more effectively, $\Delta\Phi^*/\Delta k$ is plotted against the length of the motionless part of the control rod oscillation cycle in figures 5 and 6. Figure 5 shows data when the rods are moved from their equilibrium position for one second; figure 6 shows data when this motion lasts two seconds. The effect of the temperature-dependent reactivity changes is shown clearly by the difference between the curve obtained at 1 mw and the curve obtained at 450 mw.

The experimental data ($\Delta\Phi^*/\Delta k$) are quite reproducible. Figure 7 shows two sets of data taken at times forty-two days (about 25,000 mwd exposure) apart. These data, which show good reproducibility, are from a different type of fuel charge (Mark II core) operating at a reactor power level of 585 mw. (Note: The data shown in figure 7 are $\Delta\Phi^*_{100}/\Delta k$ instead of $\Delta\Phi^*_{75}/\Delta k \equiv \Delta\Phi^*/\Delta k$.)

## Interpretation of Data

The technical complexity of the conditions under which the data were obtained necessitates analysis something less that straightforward. The successful procedure is to fit a theoretical curve to the experimental data shown in figures 5 and 6, using as adjustable parameters $\Lambda$, the thermal time constant of the fuel $\gamma_f$, and the thermal time constant of the moderator $\gamma_m$. The nature of the physico-mathematical problem is such that each of these three parameters has a distinct, easily separable effect, so that each can be determined uniquely.

Calculations. The calculations provide a detailed description of the flux as a function of time. They are based on a set of coupled differential equations describing the behavior with time of thermal neutron density, delayed neutron precursor densities, and temperatures of reactor components. A solution to these equations, in the form of an expansion in sinusoidal functions, is shown in appendix C. The solution requires the following assumptions:

- The flux distribution in the reactor is determined by the equation $\nabla^2\phi + B^2\phi = 0$, with $B^2$ constant throughout the reactor, and remains unchanged by the oscillations.

- Transient effects die out rapidly, so that variables can be expressed in terms of periodic functions of time only. A more detailed mathematical analysis, performed by H. D. Brown of the Savannah River Laboratory and currently being prepared for publication, shows that the transient contributions are negligible after about $1\frac{1}{2}$ full cycles.

- Second order terms in flux, reactivity, and temperature changes are zero. The analysis by Brown shows that almost no error is incurred by making this assumption.

- The temperature coefficients of $\Sigma_a)_{eff}$ in the reactor are at most 1% of the coefficients of the natural variable $k_\infty\Sigma_a)_{eff}$. This value is an estimated upper limit. However, the completed calculations show (1) that moderator temperature changes are so small for the oscillations used (ie, $\gamma_m/\gamma_f \ll 1$) that their effect on flux response is negligible, and (2) that even if the fuel temperature coefficient of $\Sigma_a)_{eff}$ is doubled (ie, is 2% of the reactivity coefficient), its effect on flux response is negligible.

There remain six essential parameters in the calculations. Of these, the values of three are sought by requiring a fit to the experimental data. These three are $\Lambda$, $\gamma_f$ and $\gamma_m$. The remaining three parameters are the moderator temperature coefficient of reactivity, and the statistically weighted average temperatures of the fuel and moderator. The moderator temperature coefficient of reactivity is measured in an independent test performed at very low power.

[redacted]

In this test, the moderator is heated by circulation pump power when the heat-exchanger cooling water flow is reduced, and the reactivity change caused by the moderator temperature change is then measured. (The reactivity measurement is made using the rod oscillation technique mentioned above. This measurement has also been made in a test facility using stable period measurements.)

The moderator temperature is measured directly by thermocouples distributed throughout the reactor. The fuel temperature and its distribution, however, must be calculated from heat transfer and conductivity coefficients, coolant flow rates and temperatures, etc. The flux distribution, which may be calculated or measured with reasonable accuracy, is then used with the calculated temperatures to obtain a weighted average fuel temperature. This quantity is the major source of uncertainty in the value of $\Lambda$ obtained from this analysis, since any error is reflected directly in $\Lambda$. (The distinct variable appearing in the calculations is the product of $\Lambda$ and the average temperature.)

The solutions express the relative flux, $\phi/\phi_o$, as a function of (time and) the driving function $\Sigma_a$. It can be shown that $\Delta k \sim -L(\Delta\Sigma_a/\Sigma_a)$, where $\Delta k$ and $\Delta\Sigma_a$ are the driving amplitudes of k and $\Sigma_a$, respectively, and L is the non-leakage probability for thermal neutrons. Thus, conversions between $\Delta k$, the measured driving function, and $\Delta\Sigma_a$, the driving function used in the calculations, can be made.

The accuracy of the calculations was tested in the limiting case of very low reactor power level, where temperature effects on pile behavior are negligible. Calculated values of $\Delta\Phi^*$ for this case are compared in table 3 with the experimental values obtained at a pile power of about 1 mw (listed in table 1). The excellent agreement in the values shown in table 3 demonstrates the adequacy of the mathematical description in this limiting case.

Results. In making comparisons of experimental and calculated values in order to determine $\Lambda$, $\gamma_f$, and $\gamma_m$, graphs of the type shown in figures 5 and 6 are convenient.

Figure 8 illustrates the effect of $\gamma_m$ on the flux response. In that figure, the parameters have the following values:

| | curve 1 | curve 2 | curve 3 |
|---|---|---|---|
| $\Lambda$, $\Delta k/°C$ | $-1.59 \times 10^{-5}$ | $-1.59 \times 10^{-5}$ | $-1.59 \times 10^{-5}$ |
| $\gamma_f$, $sec^{-1}$ | 0.341 | 0.341 | 0.341 |
| $\gamma_m$, $sec^{-1}$ | 0.05 | 0.028 | 0 |

[redacted]

Comparison of these curves with the experimental curve included for reference shows that a very small $\gamma_m$, effectively zero for these calculations, allows the best fit. (The final choice of parameters and the successful fit bears this out.) $\gamma_m = 0$ means that the "thermal inertia" of the moderator system is very large in these tests, and that consequently the effect of moderator temperature coefficients is very small (zero in the calculations).

Figure 9 illustrates the effect of $\gamma_f$ on the flux response. In that curve, the parameters have the following values:

| | curve 1 | curve 2 | curve 3 | curve 4 |
|---|---|---|---|---|
| $\Lambda$, $\Delta k/°C$ | $-1.59 \times 10^{-5}$ | $-1.59 \times 10^{-5}$ | $-1.59 \times 10^{-5}$ | $-1.59 \times 10^{-5}$ |
| $\gamma_f$, $sec^{-1}$ | 0.341 | 0.25 | 0.4 | 0.35 |
| $\gamma_m$, $sec^{-1}$ | 0.028 | 0.028 | 0 | 0 |

Curves 1 and 2 show that the response is sensitive to $\gamma_f$, and that the response is affected in a different way than by $\gamma_m$. Curves 3 and 4, which are more compatible with the experimental data, show that $\gamma_f = 0.35$ $sec^{-1}$ is too small, and indicate that $\gamma_f$ is about 0.4 $sec^{-1}$, or slightly larger.

A simple computation using the equilibrium statement of $\gamma_f$, power and temperatures required by the temperature equation used in these calculations (ie, by the boundary condition) gives $\gamma_f = 0.341$ $sec^{-1}$. The fact that this value of $\gamma_f$ does not give a satisfactory fit shows that the temperature equation used does not give a wholly adequate model of fuel temperature behavior. However, when the available equation is used with a value of $\gamma_f$ determined from comparisons with experimental data, the description of temperature behavior is adequate so long as no variable becomes very different in magnitude.

Figure 10 shows the effect of $\Lambda$ on the flux response. In that figure, the parameters have the values:

| | curve 1 | curve 2 | curve 3 |
|---|---|---|---|
| $\Lambda$, $\Delta k/°C$ | $-1.59 \times 10^{-5}$ | $-1.22 \times 10^{-5}$ | $-0.61 \times 10^{-5}$ |
| $\gamma_f$, $sec^{-1}$ | 0.341 | 0.341 | 0.341 |
| $\gamma_m$, $sec^{-1}$ | 0.028 | 0.028 | 0.028 |

These curves indicate that $\Delta\Phi^*/\Delta k$ is quite sensitive to $\Lambda$, and that it is affected by $\Lambda$ in a way different from either $\gamma_m$ or $\gamma_f$.

[redacted]

Figures 8, 9, and 10 show that $\gamma_m$ affects the shape of the response curve at long "period" times, predominantly; $\gamma_f$ affects the shape of the response curve at short "period" times, predominantly; and $\Lambda$ affects the level of the response curve, predominantly. When the three parameters were adjusted to the experimental data simultaneously, it was found that the same set would not fit the curves with one and two-second rod motions (from equilibrium) at the same time. Therefore, two distinct sets of parameters were obtained, one set fitting the one-second data and the other set fitting the two-second data. The curves are shown in figures 11 and 12. Curve 1 uses $\gamma_m = 0$, $\gamma_f = 0.475$ $sec^{-1}$, $\Lambda = -1.22 \times 10^{-5}$ $\Delta k/°C$, and fits the one-second experimental data shown in figure 11. Curve 2 uses $\gamma_m = 0$, $\gamma_f = 0.4$ $sec^{-1}$, $\Lambda = 1.40 \times 10^{-5}$ $\Delta k/°C$ and fits the two-second experimental data shown in figure 12. The best value of $\gamma_f$ is then 0.438 $sec^{-1}$ with a precision of ± 9%, and the best value of $\Lambda$ is $-1.3 \times 10^{-5}$ $\Delta k/°C$ with a precision of ± 7%.

## Conclusions

Synopsis. In order to measure $\Lambda$, oscillate calibrated control rods on a truncated sawtooth cycle, and measure the temperature-sensitive part of the flux response. It is then required that the calculations agree with the measurements, which determines $\Lambda$ and the thermal time constants of fuel and moderator independently, because of their distinguishable effect on cycles of different shape and length. The primary source of error is in the value of equilibrium fuel temperature used in the equations. Error from this source could be as high as ± 15%.

A secondary source of error which has not been examined quantitatively is the redistribution of flux during the oscillations. During the "period" part of the flux response, the hottest fuel elements have the highest statistical weight. This condition tends to decrease the amplitude of the effective temperature change in the negative half-cycle, and increase it in the positive half-cycle. Of course, after transients have passed, the oscillations occur about the equilibria. The error caused by neglecting this effect is probably small.

Applicability of Technique. The method can be applied to any reactor which can be analytically homogenized, in which only one temperature-reactivity parameter is unknown, and in which the time constants of important components are either known or differ widely. However, the kinetics of a reactor having two or more regions with widely different properties are more complicated. Interpretation of oscillation data in a two-region reactor at Savannah River by kinetics calculations of this type have resulted in values of $\Lambda$ with wide limits of error (perhaps ± 50%).

[redacted]

Acknowledgments. The general features of the technique were originally conceived by E. W. Hones, Jr.

H. D. Brown of the Savannah River Laboratory supplied an independent development of the solutions to the set of differential equations, and evaluated the parameters for the cases considered in this report using the IBM-650 computer.

## Bibliography

1. Lapsley, A. C., Differential Electrometer, DP-95, December 1954.

2. Glasstone and Edlund, The Elements of Nuclear Reactor Theory, D. Van Nostrand Company Inc., New York, 1952.

SCL:mhg

# Tables and Figures

## Tables



## Figures

Table 1

Experimental Values of $\Delta\Phi^*/\Delta k$
(Reactor Power - 1 mw)

A. Rod Motion from equilibrium - 1 sec

| Motionless Period, sec | % $\Delta k$ | % $\Delta\Phi^*$ | $\Delta\Phi^*/\Delta k$ |
|---|---|---|---|
| 1 | 0.00435 | 0.167 | 38.4 |
| 2 | 0.00432 | 0.214 | 49.5 |
| 4 | 0.00461 | 0.380 | 82.4 |
| 6 | 0.00448 | 0.502 | 112. |
| 8 | 0.00457 | 0.619 | 135. |

B. Rod Motion from equilibrium - 2 sec

| Motionless Period, sec | % $\Delta k$ | % $\Delta\Phi^*$ | $\Delta\Phi^*/\Delta k$ |
|---|---|---|---|
| 1 | 0.00815 | 0.155 | 19.0 |
| 2 | 0.00894 | 0.370 | 41.4 |
| 4 | 0.00892 | 0.661 | 74.1 |
| 6 | 0.00898 | 0.955 | 106. |
| 8 | 0.00909 | 1.15 | 127. |
| 10 | 0.00886 | 1.35 | 152. |

Table 2

Experimental Values of $\Delta\Phi^*/\Delta k$
(Reactor Power - 450 mw)

A. Rod Motion from equilibrium - 1 sec

| Motionless Period, sec | % $\Delta k$ | % $\Delta\Phi^*$ | $\Delta\Phi^*/\Delta k$ |
|---|---|---|---|
| 1 | 0.00506 | 0.0606 | 12.0 |
| 2 | 0.00562 | 0.124 | 22.0 |
| 4 | 0.00510 | 0.163 | 32.0 |
| 6 | 0.00512 | 0.223 | 43.5 |
| 8 | 0.00523 | 0.296 | 56.6 |
| 10 | 0.00524 | 0.324 | 61.8 |

B. Rod Motion from equilibrium - 2 sec

| Motionless Period, sec | % $\Delta k$ | % $\Delta\Phi^*$ | $\Delta\Phi^*/\Delta k$ |
|---|---|---|---|
| 1 | 0.01054 | 0.107 | 10.1 |
| 2 | 0.01067 | 0.187 | 17.5 |
| 4 | 0.01081 | 0.266 | 24.6 |
| 6 | 0.01072 | 0.430 | 40.1 |
| 8 | 0.01080 | 0.414 | 38.3 |
| 10 | 0.01103 | 0.520 | 47.1 |

Table 3

Calculated Values of $\Delta\Phi^*/\Delta k$
(Reactor Power - 1 mw)

A. Rod Motion from equilibrium - 1 sec

| Motionless Period, sec | $\Delta\Phi^*/\Delta k$ Calculated | $\Delta\Phi^*/\Delta k$ Experimental |
|---|---|---|
| 1 | 27.1 | 38.4 |
| 2 | 47.5 | 49.5 |
| 4 | 80.0 | 82.4 |
| 6 | 107. | 112. |
| 8 | 129. | 135. |

B. Rod Motion from equilibrium - 2 sec

| Motionless Period, sec | $\Delta\Phi^*/\Delta k$ Calculated | $\Delta\Phi^*/\Delta k$ Experimental |
|---|---|---|
| 1 | 24.2 | 19.0 |
| 2 | 43.4 | 41.4 |
| 4 | 74.0 | 74.1 |
| 6 | 100. | 106. |
| 8 | 124. | 127. |
| 10 | 148. | 152. |

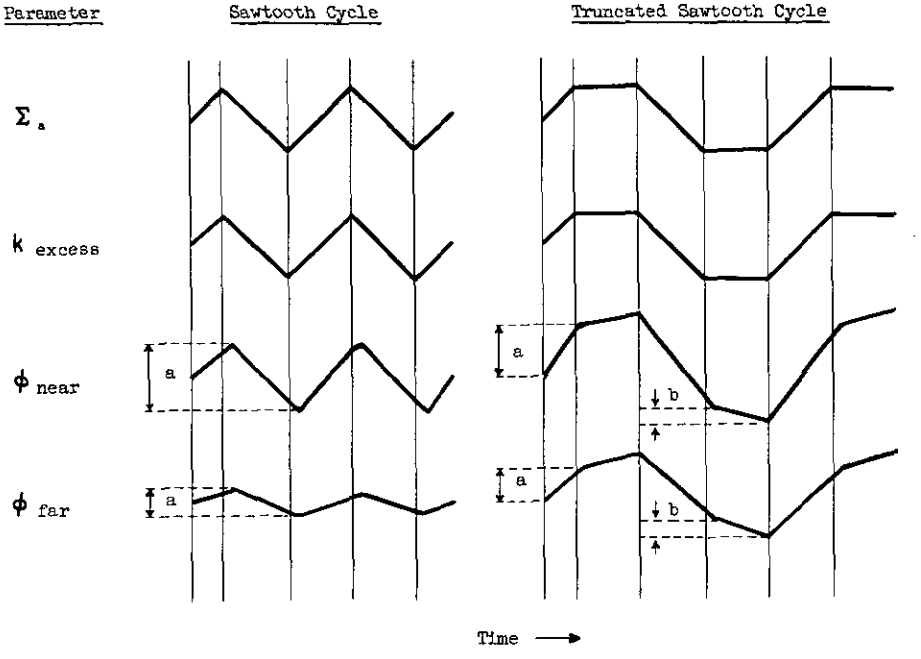


a This amplitude is strongly dependent on the spatial relationship between oscillatory $\Sigma_a$ and the position of flux measurement.

b This amplitude, called the "period" rise or fall, is usually smaller than amplitude a, and is independent of the relationship between oscillatory $\Sigma_a$ and the position of flux measurement.

**Figure 1. VARIATION OF REACTOR PARAMETERS WITH TIME**

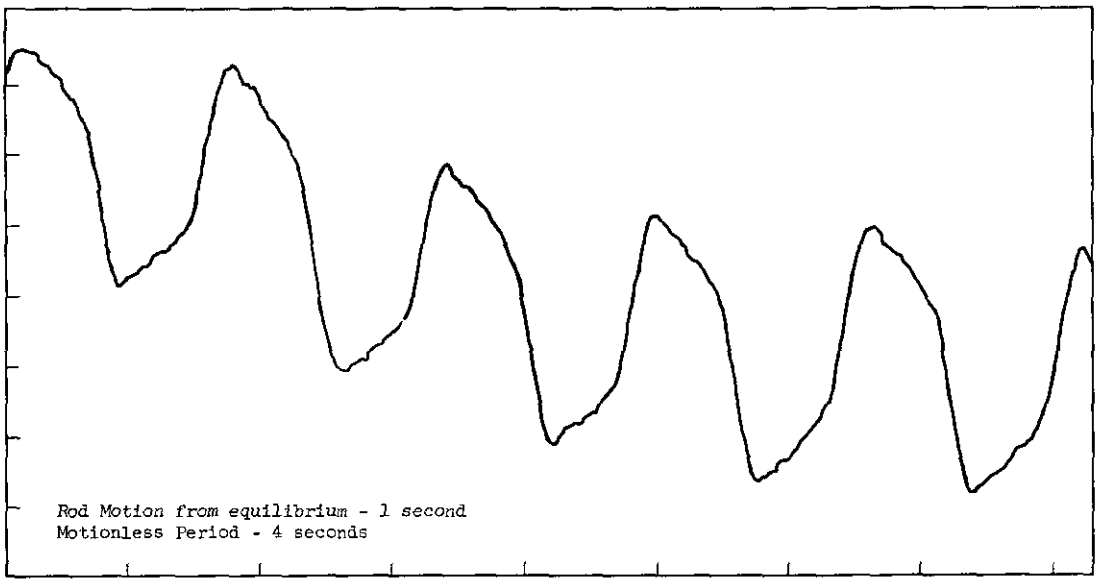


Figure 2. FLUX RESPONSE AT 1 MW

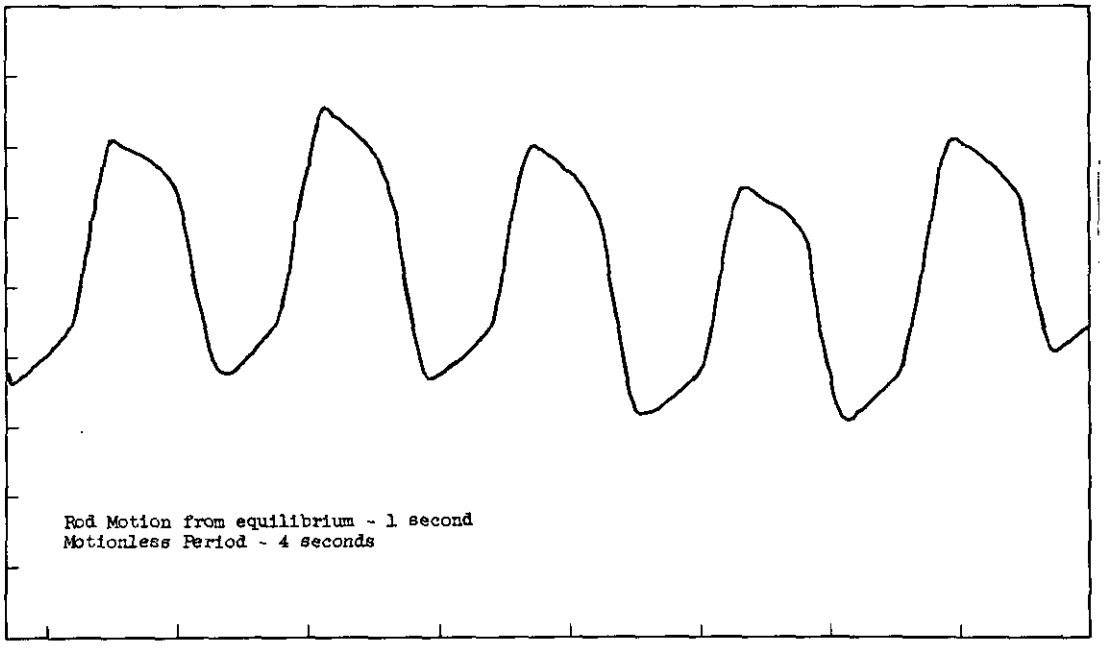


Figure 3. FLUX RESPONSE AT 450 MW

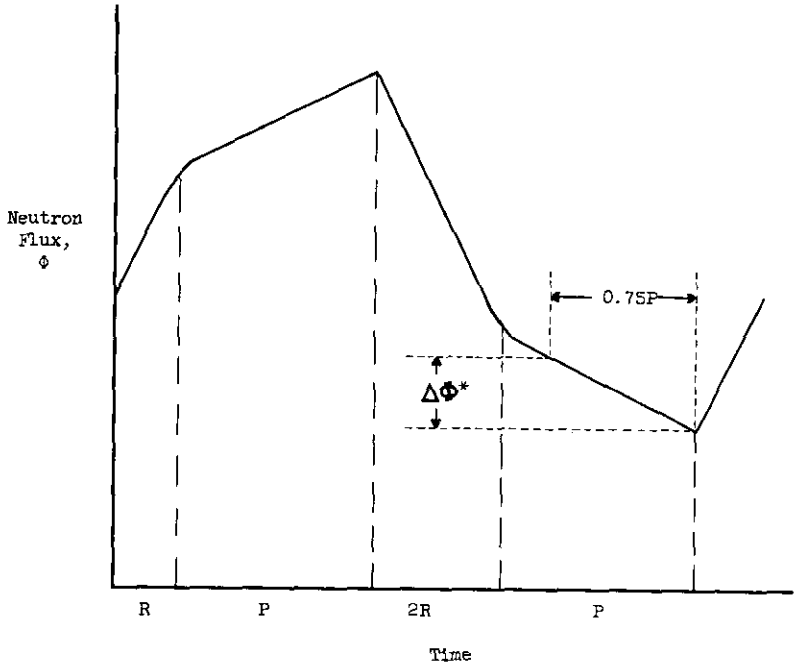


This is a typical cycle in which the control rods are raised for R seconds, held motionless for P seconds, lowered for 2R seconds, held for P seconds, raised for 2R seconds, etc

Figure 4. MEASUREMENT OF $\Delta\Phi^*$

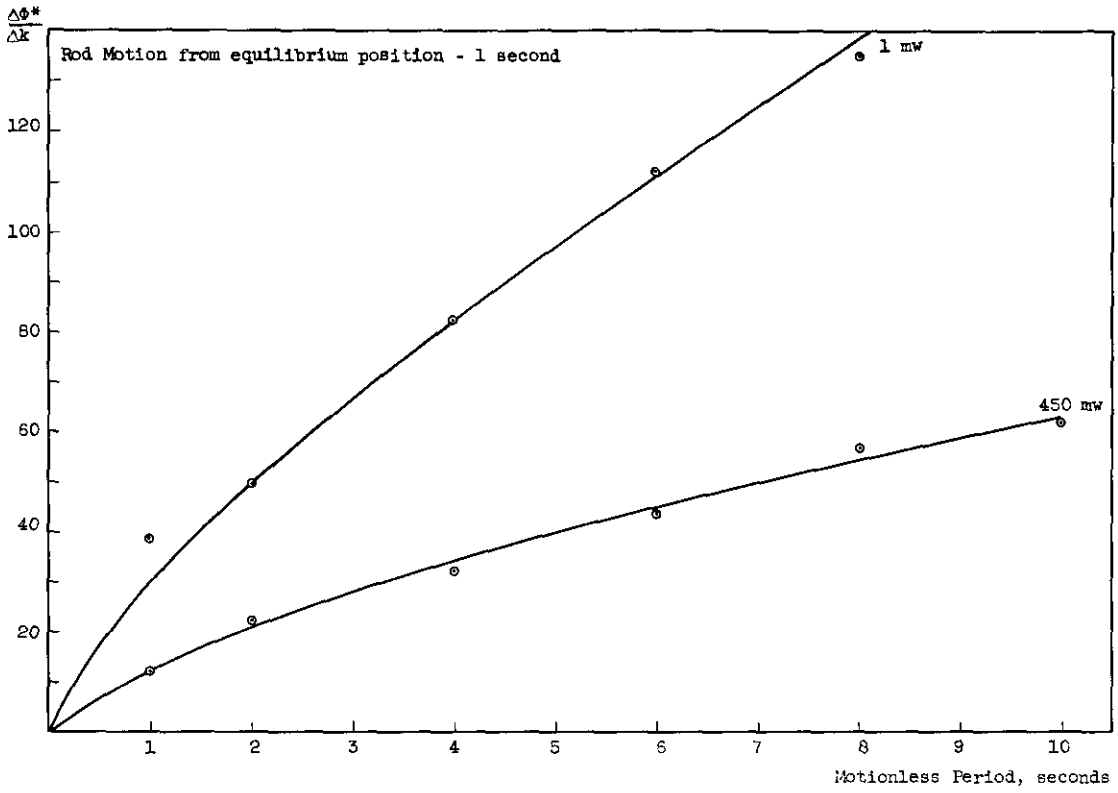


Figure 5. FLUX RESPONSE AT HIGH AND LOW POWER LEVELS

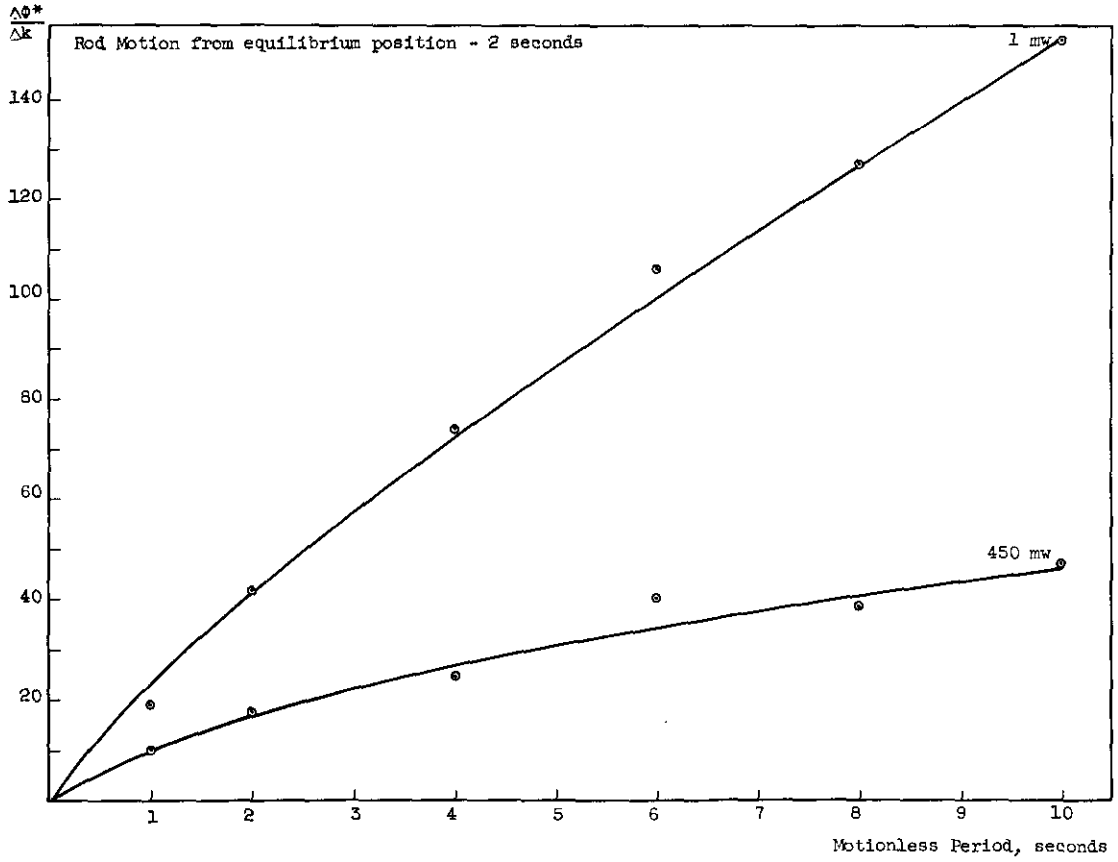


Figure 6. FLUX RESPONSE AT HIGH AND LOW POWER LEVELS

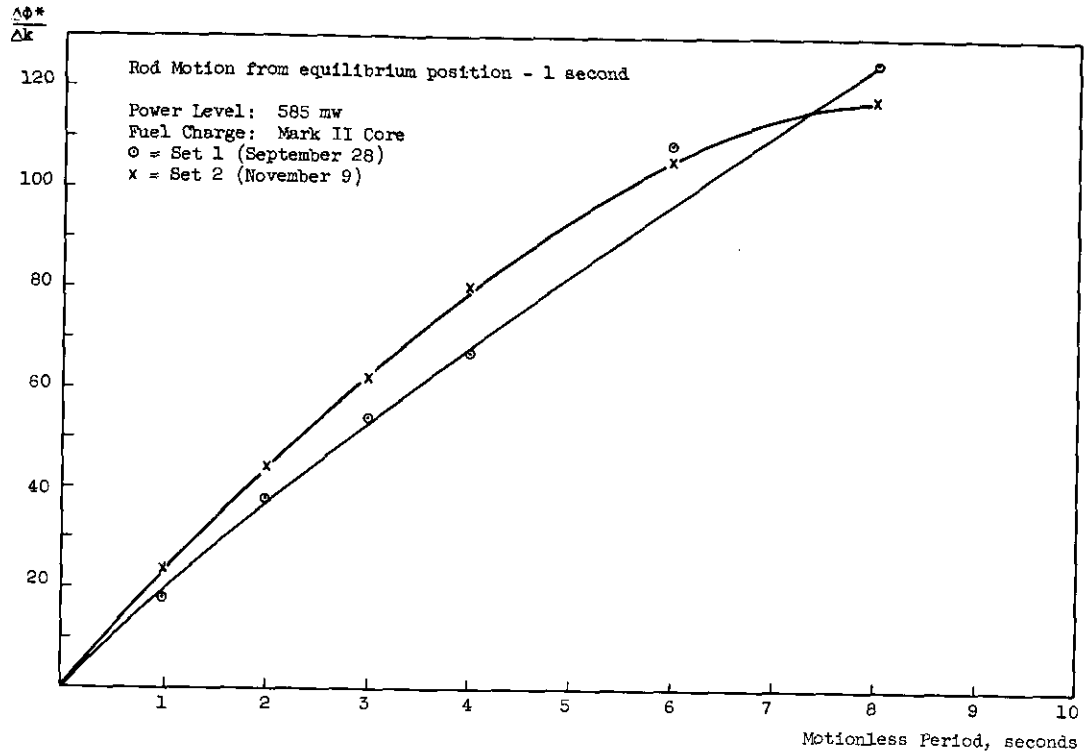


Figure 7. REPRODUCIBILITY OF DATA

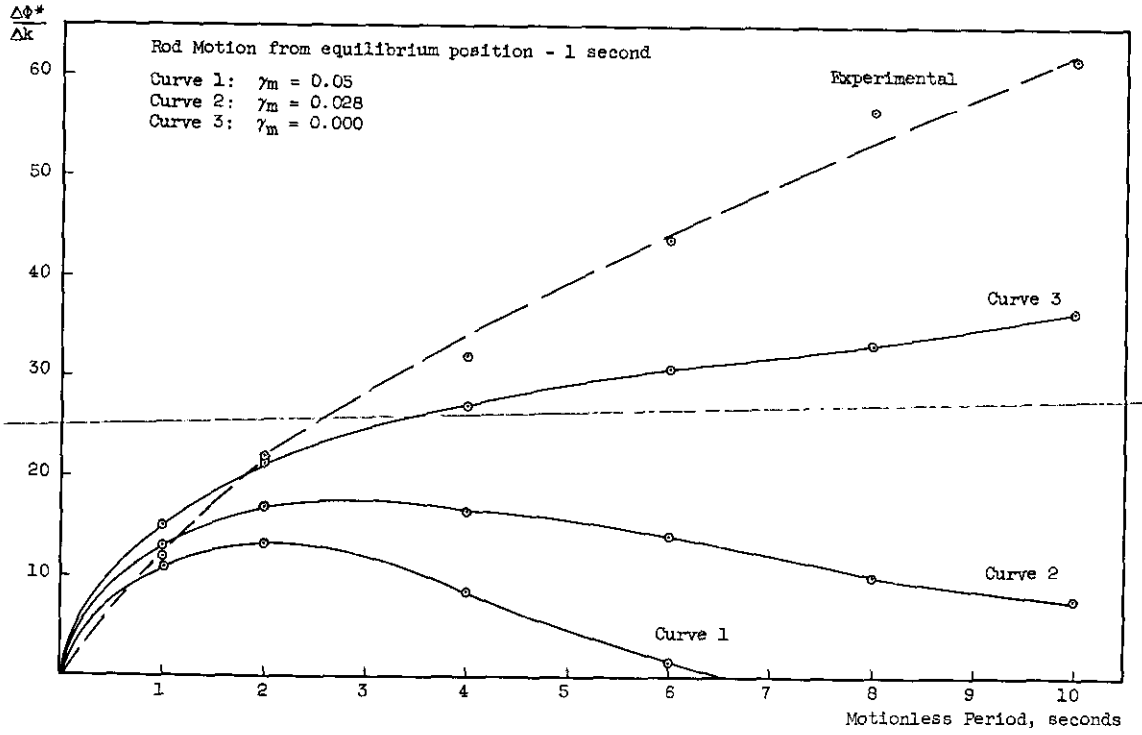


Figure 8. EFFECT OF $\gamma_m$ ON FLUX RESPONSE

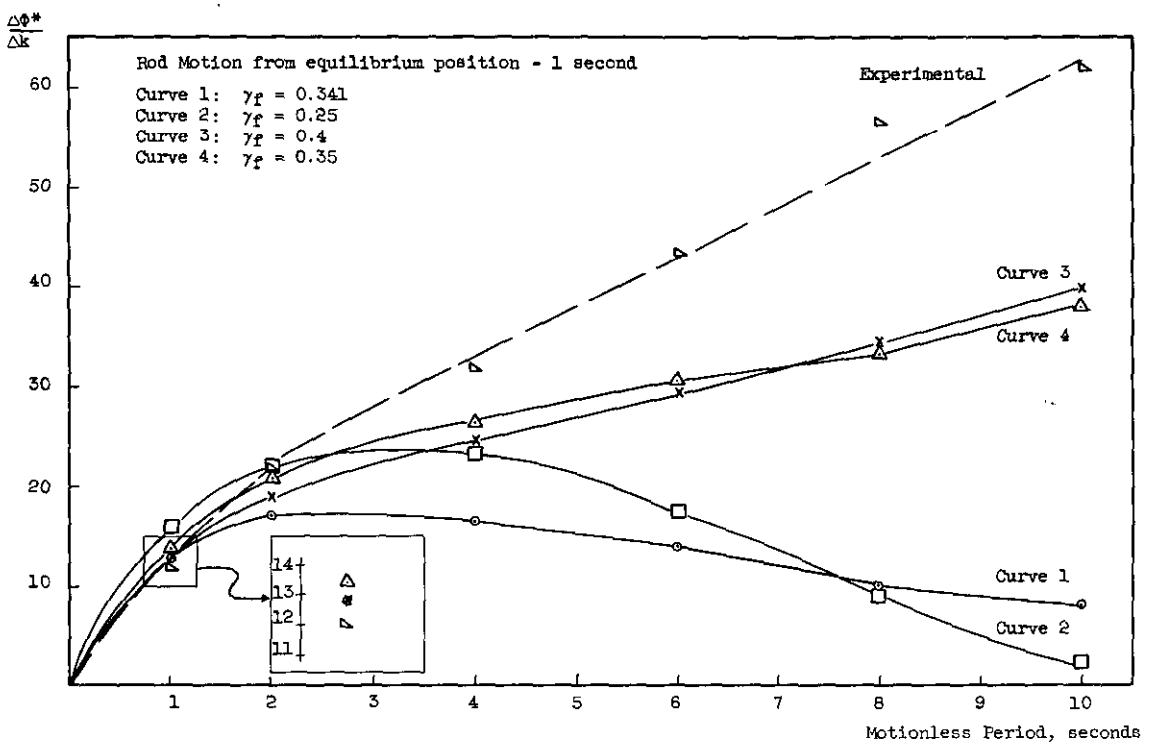


Figure 9. EFFECT OF $\gamma_f$ ON FLUX RESPONSE

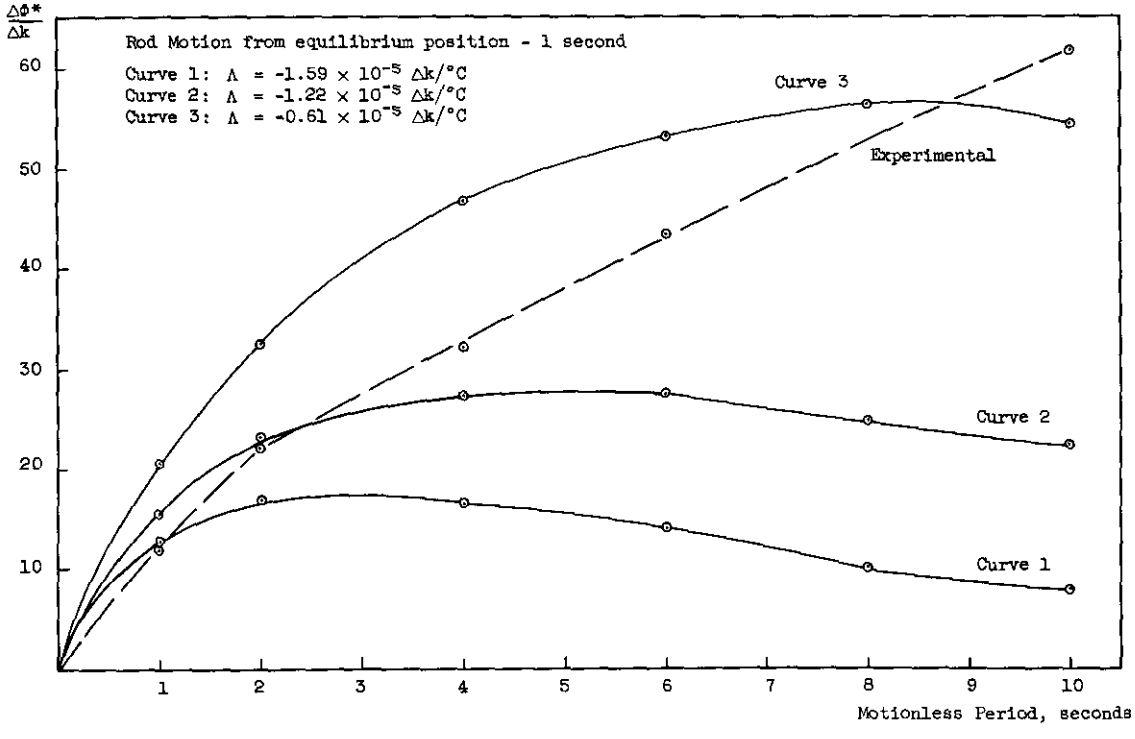


Figure 10. EFFECT OF Λ ON FLUX RESPONSE

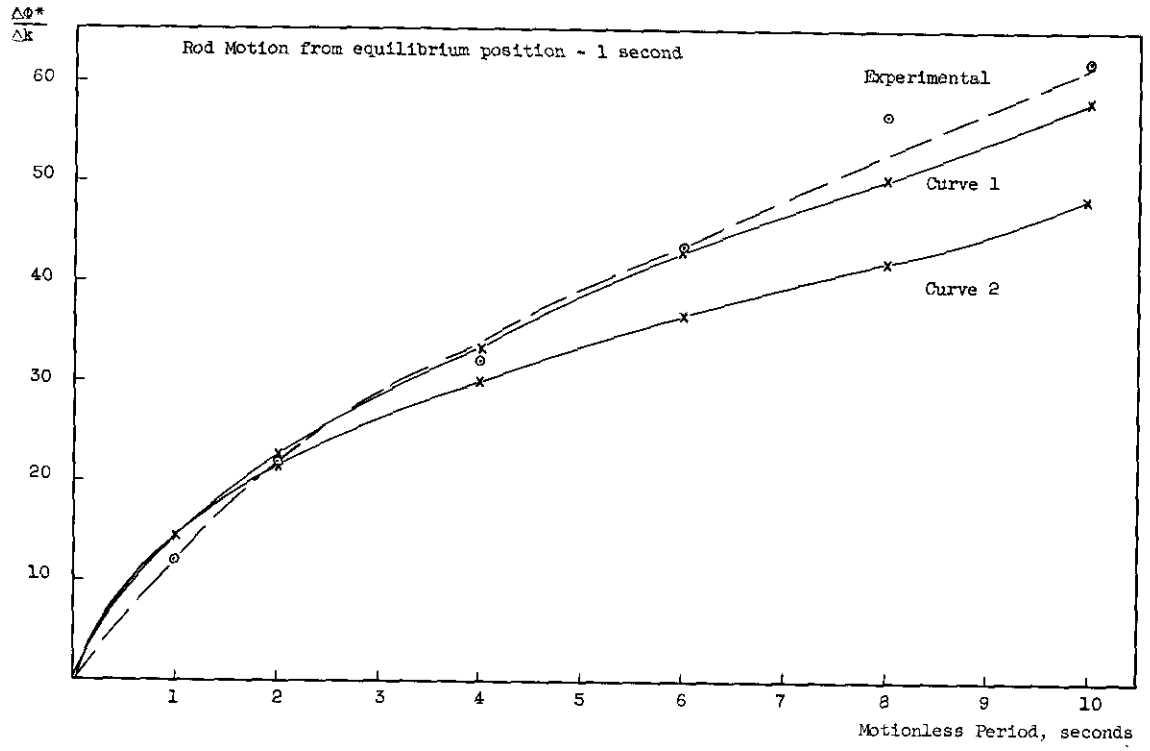


Figure 11. BEST FIT TO EXPERIMENTAL DATA

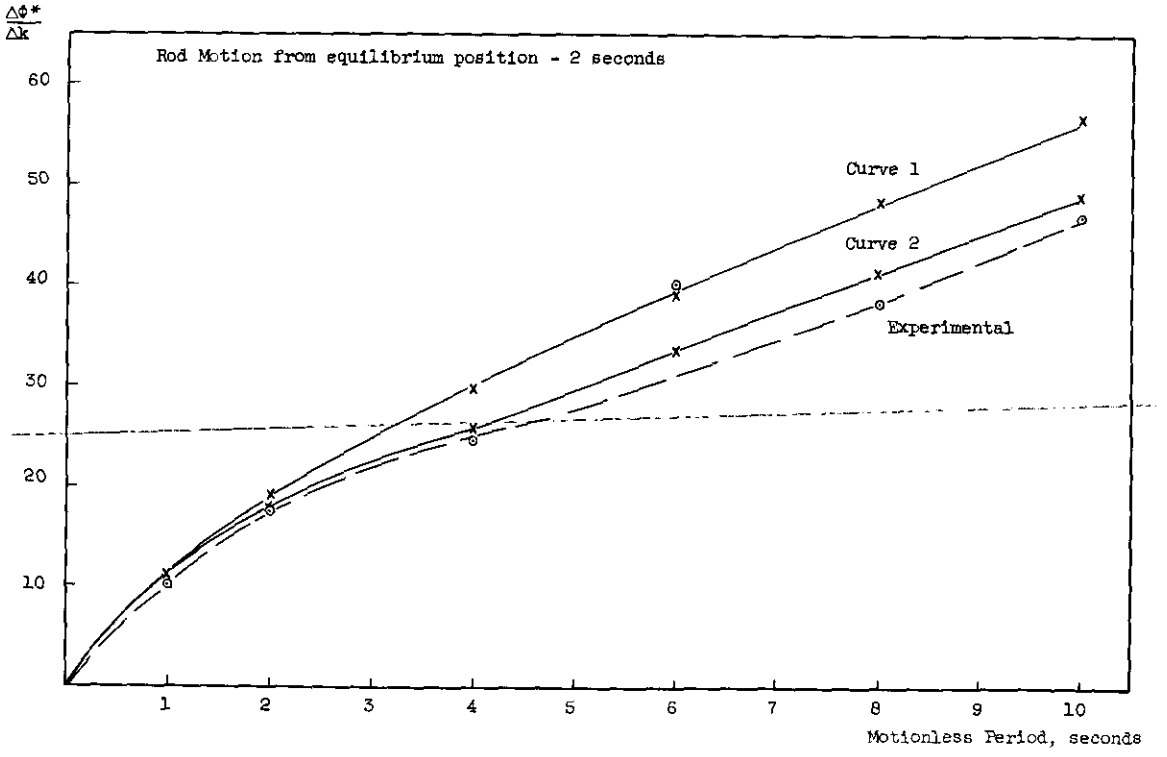


Figure 12. BEST FIT TO EXPERIMENTAL DATA

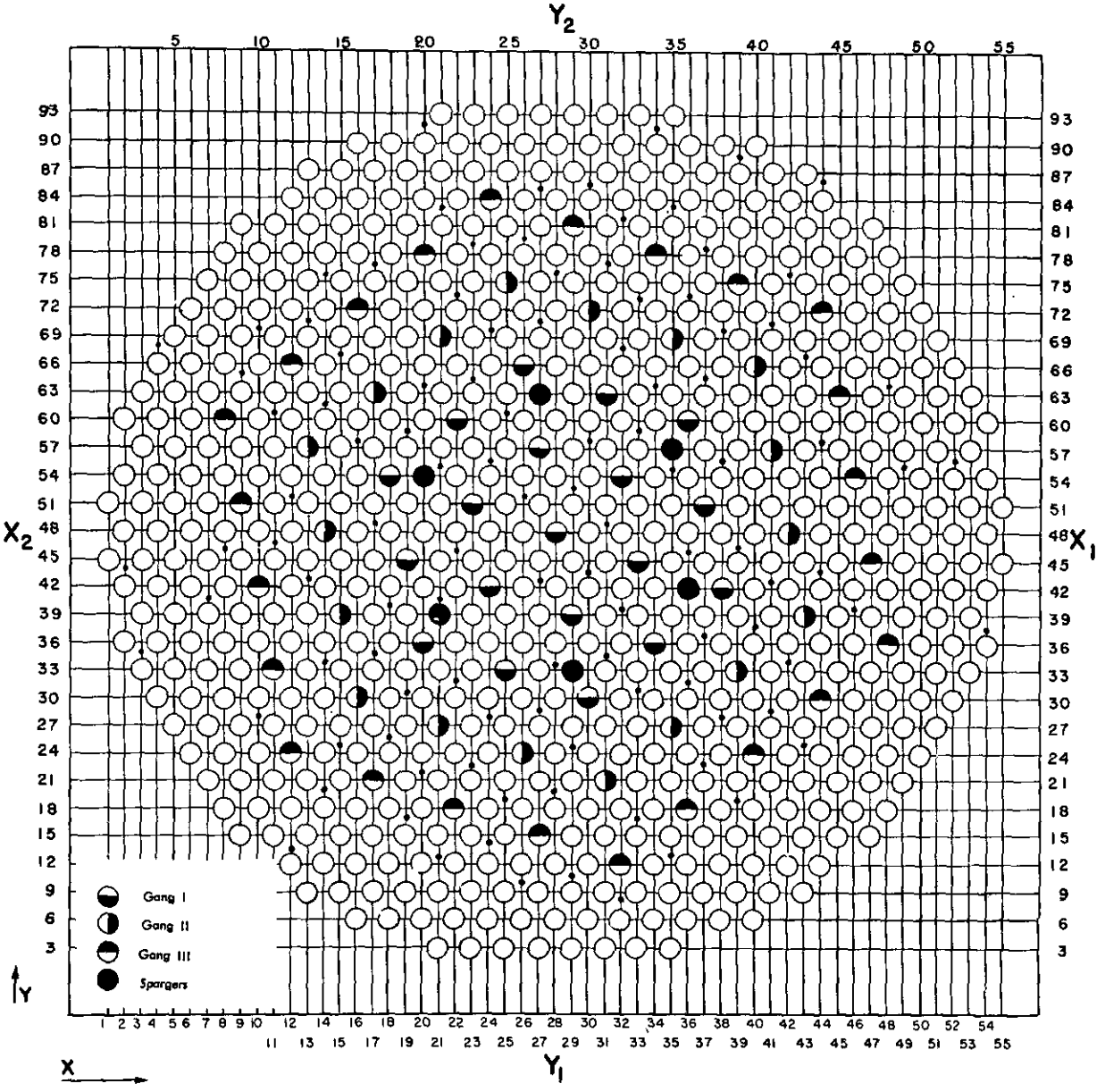


FIGURE 13. SAVANNAH RIVER REACTOR LATTICE GEOMETRY

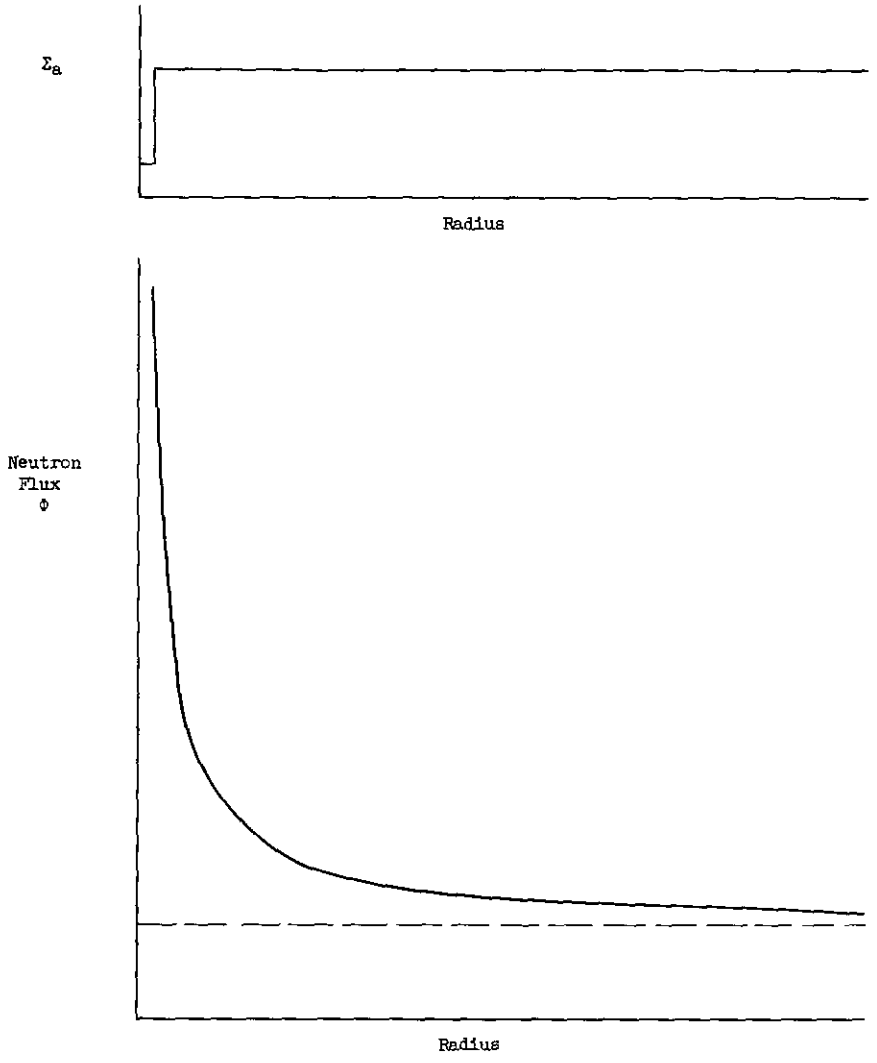


Figure 14. FLUX RESPONSE TO LOCALIZED STEP-FUNCTION IN $\Sigma_a$

# Appendix

## A. Description of a Savannah River Plant Reactor

Lattice Geometry. The extrapolated height and radius of this cylindrical reactor are 460 and 251 centimeters, respectively. Six hundred quatrefoil fuel elements and 61 septifoil control elements extend from top to bottom of a cylindrical tank filled with $D_2O$ moderator-coolant. The lattice geometry, shown in figure 13, is hexagonal, with a lattice spacing of 7 inches. Each fuel element is a quatrefoil containing four columns of fuel slugs; each control element is a septifoil containing two half-length control rods and five full-length control rods.

Lattice Composition. The fuel slugs (Mark I) are made of natural uranium and are jacketed with aluminum. The five control rods which may be used in normal operation are made of a lithium-aluminum alloy, containing 3.5% lithium by weight. Two full-length cadmium rods in each septifoil are reserved for reactor shutdown. The quatrefoil and septifoil assemblies are aluminum. The moderator-coolant is $D_2O$ whose isotopic purity is about 99.6%.

Cooling System. Heat is removed from the reactor by the circulating $D_2O$. The $D_2O$ is forced down the quatrefoils through annuli surrounding the fuel slugs, and is then allowed to circulate freely within the reactor tank until it leaves via one of six symmetrically spaced pipes at the bottom of the outer periphery of the tank. After being cooled in heat exchangers, the water returns to the top of the reactor tank. About 180 tons of water are circulated at a rate of about 85,000 gallons per minute.

Control System. The rods in the 61 control clusters provide a flexible system for reactor control and for adjustment of the neutron flux distribution. The rods, which drive into the control clusters sequentially, can be individually positioned (vertically) with an accuracy of 0.1 inch. Their position is indicated on the reactor operating console in units of 0.2 inch. In normal operation, the two half-length rods remain in the reactor for vertical flux shaping, while the full-length rods are used for control. The 61 clusters are divided into three groups, or gangs, which are controlled as units for radial flux shaping. Figure 13 shows the three control rod gangs. All control rods are remotely operated from the reactor control console, and normally move with a speed of about three centimeters per second.

Since Gang I (the central gang) can be worth as much as $7 \times 10^{-5}$ $\Delta k/cm$, reactivity can be changed using Gang I at a maximum rate of about $2 \times 10^{-4}$ $\Delta k/sec$. Withdrawing Gang I from its critical position for two seconds can put the reactor on a minimum rising stable period of about 260 seconds.

Neutron Flux Monitor. For the measurements described in this report, the thermal neutron flux is measured with a Westinghouse compensated ion chamber located at the midplane of the reactor in the iron-water thermal shield, 25 inches outside the reactor tank wall. Current from this chamber is recorded by an instrument provided with a "bucking" voltage to cancel out the major, constant portion of the signal, so that small variations may be seen easily. This instrument, called the differential electrometer, is described in detail by A. C. Lapsley in DP-95.

## B. Response of a Savannah River Reactor to Absorber Oscillations

Step-Function: Uniform Absorber. When a uniformly distributed thermal neutron absorber is decreased instantaneously, the thermal neutron flux increases very rapidly for a short time. This rapid increase is due partly to the presence of the extra neutrons which are no longer being absorbed, and partly to multiplication of the "prompt" neutrons. Following this initial change, the number of neutrons multiplies slowly.

If the reactor power is high enough that increases in temperature due to the increasing power can cause sensible changes in the neutron multiplication constant, a stable doubling time is not reached. Because the flux changes slowly, at a rate determined by the excess reactivity of the system, and because this reactivity would otherwise be fixed, the reactivity changes due to temperature increases have a distinct, mensurable effect on the flux behavior.

In a heterogeneous reactor, the temperature of each component may be different and will, in general, have a different effect on pile reactivity. Furthermore, the thermal relaxation times of the various components may differ widely. In particular, the thermal relaxation time may be ten times or more as large for the moderator as for the fuel. (This is actually the case in a Savannah River reactor.)

If, in a heterogeneous reactor, the time constants of the temperatures of the reactor components differ widely, temperature effects on the flux rise will at first be due largely to components with short time constants. The effects due to those components with longer time constants will increase in magnitude as time goes on. In a Savannah River reactor, the fuel temperature following a step change in power undergoes about 67% of its total change in three seconds, while the moderator temperature has experienced less than 5% of its total change. Thus, the two effects are chronometrically separable to a high degree.

Step-Function: Localized Absorber. When the absorption in a small region is decreased instantaneously, the immediate neutron response in the region of the absorption change is very nearly the same as in the case of the uniformly distributed absorber. However, the neutron population elsewhere is changed only by the appearance of neutrons leaking out of the region of absorption change. This diffusion occurs very rapidly, so that the neutron behavior immediately following the absorption change can be viewed as a simple redistribution of the neutron flux concomitant with a small over-all increase in the power.

If the flux distribution before the absorption change was uniform, the new distribution will be like that shown in figure 14. At least in the first approximation, the distribution will be a stable one, determined by the usual equilibrium conditions. The total increase in reactor power is very nearly the same as if a uniformly distributed absorber of equivalent strength were decreased.

Following this rapid redistribution, the neutron population multiplies slowly, in much the same way as when the absorber change was uniform throughout the reactor. The new flux distribution is maintained as the over-all level increases, so that the fractional increase is uniform over the reactor, as before.

To summarize, the primary difference in the flux response due to a step-change in a localized absorber, compared to that in a uniformly-distributed absorber, is that the slow "period" rise of the flux is from a distorted distribution caused by the nonuniform poison distribution. During the "period" rise of the flux, the flux and temperature changes in each component, averaged over the volume of the reactor, are nearly the same in both cases. Furthermore, the flux and temperature changes during the "period" rise are fractionally uniform throughout the reactor.

Oscillation of a Localized Absorber - Applications.

1. Sawtooth Oscillation Cycle - For an 8-second sawtooth cycle, the flux response in a Savannah River reactor to an oscillating localized absorber is (a) approximately independent of reactor power level, (b) approximately proportional to the reactivity change caused by the oscillating absorber, and (c) a strong function of the geometrical position of the absorber and the position at which the flux response is measured.

   The independence of reactor power level results from two facts. First, the moderator temperature changes are small (because of the long temperature time-constant), so that power-dependent reactivity effects are small (the moderator temperature is otherwise a major contributor). Secondly, throughout the cycle, $k_{ex}$ of the system is changing (a direct consequence of the absorber motion) with an amplitude large compared to possible temperature-reactivity effects.

   The proportionality of the flux response to the amplitude of the oscillating $k_{ex}$ is due to the smallness of the changes.

   The dependence of the flux response on position relative to the absorber is a result of the redistribution of the neutron flux concomitant with the general rise and fall of power (see "Step-Function: Localized Absorber" page 26). Figure 1 shows $\Sigma_a$, $k_{ex}$, and $\phi$ as a function of time for a sawtooth cycle.

A reliable "oscillation technique" has been developed by means of which the worth of control rods at any position, at any power level, may be determined from (1) a set of empirical calibration curves, and (2) the flux oscillation amplitude resulting from oscillation of the subject control rods on an 8-second sawtooth cycle.

The calibration curves are obtained experimentally at zero reactor power from stable period measurements and representative control rod oscillations. These curves are, of course, approximately independent of power level, oscillatory $\Delta k$ amplitude, and fuel or control rod burnout. They show the ratio of flux response amplitude to oscillatory $\Delta k$ amplitude, for control rod tips at varying positions with respect to the flux monitor. The curves are greatly simplified by the fact that, to a first approximation, the ratio $(\Delta\phi/\phi)/\Delta k$ depends only on the distance between control rod tip and flux monitor, and not on the geometry of the system.

2. Truncated Sawtooth Oscillation Cycle - This cycle is the practical form of a square wave, which is a series of alternating step-functions of the type discussed above (page 26). The same characteristics as the step-function are shown by oscillations of this type. Figure 1 shows $\Sigma_a$, $k_{ex}$, and $\phi$ as a function of time for a truncated sawtooth cycle.

Thus, when a localized absorber is oscillated in this way anywhere in the reactor, the "period" rise or fall of the neutron flux will be independent of the position of the absorber, and will be sensitive to reactivity changes caused by changes in the temperatures of the reactor components. Furthermore, if the cycle length is restricted to a few seconds, these reactivity changes will be due predominantly to fuel temperature changes. Therefore, if fuel temperature behavior is known, proper interpretation of the measured flux response to oscillations of this type in a reactor operating at a relatively high power level will provide a value of $\Lambda$ .

## C. Calculations*

For thermal neutrons, delayed neutron precursors, and reactor component temperatures, we write the following equations:**

$$D\nabla^2\phi - \Sigma_a\phi + \Sigma_a\phi\,(1-\beta)k_\infty e^{-\tau B^2} + pe^{-\tau B^2}\sum_i \lambda_i c_i = \left(\frac{\dot{\phi}}{v}\right)$$

$$\dot{c}_i = f_i\,\frac{\beta k_\infty}{p}\,\Sigma_a\phi - \lambda_i c_i$$

$$\dot{\theta}_j = M_j\phi - \gamma_j\theta_j$$

where: $f_i \equiv \beta_i/\beta$

$\gamma_j \equiv$ thermal relaxation constant $(\sec^{-1})$ of the $j^{th}$ component

$M_j \equiv$ a constant of proportionality

$\theta \equiv$ the temperature above zero-power temperature

For convenience, define $k_\infty \equiv ab$, where $b \equiv \Sigma_{a_o}/\Sigma_a$.

Then divide variables by their steady state value and subtract 1:

$$\Phi \equiv (\phi/\phi_o) - 1,\quad C \equiv (c/c_o) - 1,\quad T \equiv (\theta/\theta_o) - 1,\quad V \equiv (v/v_o) - 1$$

Thus the equations become:

$$\dot{\Phi} = A\Phi + B\sum_i f_i C_i + A + B$$

$$C_i = \lambda_i\,\{a\Phi - C_i + (a-1)\}$$

$$\dot{T}_j = \gamma_j\,(\Phi - T_j)$$

where: $A \equiv \dfrac{1-\beta}{\beta}\,aB - (1 + bL_o^2B^2)\,\dfrac{(V+1)}{\ell_o b} + \dfrac{\dot{V}}{(V+1)}$

$$B \equiv \beta\,(1 + L_o^2B^2)\,\frac{V+1}{\ell_o}$$

($\ell_o \equiv 1/v\Sigma_a$, the thermal neutron lifetime in a reactor without leakage)

---

* Assumptions are listed on page 5 of the text.

** See reference 2, page 9.

The temperature coefficients of the variables a and b are $\alpha_j$ and $\mu_j$, respectively. With the assumption that the temperature variations are sufficiently small that a linear approximation is adequate, $\alpha_j$ and $\mu_j$ appear as follows:

$$a = 1 + \sum_j \alpha_j T_j$$

$$b = 1 - F - \sum_j \mu_j T_j$$

(Here F is the impressed driving function in $\Sigma_{ao}/\Sigma_a$)

It can be shown that, to a very good approximation,

$$\Lambda_j = \frac{1}{\theta_{oj}} \{\alpha_j - \mu_j/(1 + L_o^2 B^2)\}$$

where $\Lambda_j$ is the temperature coefficient of reactivity ($\Delta k/°C$) of the $j$th reactor component.

The neutron velocity is proportional to the square root of the moderator temperature, so that

$$V + 1 = [1 + T_{mod}/K]^{\frac{1}{2}} \sim 1 + T_{mod}/2K$$

$$V \sim T_{mod}/2K$$

where $K \equiv 1 + h/\theta_{o)\ mod}$, and h is the zero-power temperature of all reactor components.

Now expand the variables as follows:

$$\Phi = \sum_k c_k e^{ik\omega t}$$

$$C_i = \sum_k b_{ik} e^{ik\omega t}$$

$$T_j = \sum_k d_{jk} e^{ik\omega t}$$

$$F = \sum_k \delta_k e^{ik\omega t}$$

$$\frac{}{V = \sum_k r_k e^{ik\omega t}}$$

Substitute these expansions into the modified equations, drop terms of order >1, and apply the conditions of orthogonality:

$$i\omega k\psi\ell_o c_k = -c_k + \sum_i f_i b_{ik} + \frac{1-\beta}{\beta} \sum_j \alpha_j d_{jk} - \psi\delta_k - \psi\sum_j \mu_j d_{jk} + i\omega k r_k \psi\ell_o$$

$$i\omega k b_{ik} = \lambda_i \left(c_k - b_{ik} + \sum_j \alpha_j d_{jk}\right)$$

$$d_{jk}\left(i\omega k + \gamma_j\right) = \gamma_j c_k$$

$$r_k = \frac{1}{2K} d_{mk}$$

(Here $\psi \equiv \beta^{-1}\left(1 + L_o^2 B^2\right)^{-1}$ and subscript m refers to moderator.)

These equations can be solved simultaneously to obtain $c_k$ in terms of $\delta_k$:

$$-\psi\delta_k c_k^{-1} = 1 - \left(1 + \sum_j \frac{\alpha_j \gamma_j^2}{\gamma_j^2 + \omega^2 k^2}\right) \sum_i \frac{f_i \lambda_i^2}{\lambda_i^2 + \omega^2 k^2}$$

$$+ \omega^2 k^2 \sum_i \frac{f_i \lambda_i}{\lambda_i^2 + \omega^2 k^2} \sum_j \frac{\alpha_j \gamma_j}{\gamma_j^2 + \omega^2 k^2} + \psi \sum_j \frac{\mu_j \gamma_j^2}{\gamma_j^2 + \omega^2 k^2}$$

$$- \frac{1-\beta}{\beta} \sum_j \frac{\alpha_j \gamma_j^2}{\gamma_j^2 + \omega^2 k^2} - \omega^2 k^2 \frac{\psi\ell_o}{2K} \frac{\gamma_m}{\gamma_m^2 + \omega^2 k^2}$$

$$+ i\omega k \left\{\psi\ell_o + \left(1 + \sum_j \frac{\alpha_j \gamma_j^2}{\gamma_j^2 + \omega^2 k^2}\right) \sum_i \frac{f_i \lambda_i}{\lambda_i^2 + \omega^2 k^2}\right.$$

$$+ \sum_j \frac{\alpha_j \gamma_j}{\gamma_j^2 + \omega^2 k^2} \sum_i \frac{f_i \lambda_i^2}{\lambda_i^2 + \omega^2 k^2} - \psi \sum_j \frac{\mu_j \gamma_j}{\gamma_j^2 + \omega^2 k^2}$$

$$\left. + \frac{1-\beta}{\beta} \sum_j \frac{\alpha_j \gamma_j}{\gamma_j^2 + \omega^2 k^2} - \frac{\psi\ell_o}{2K} \frac{\gamma_m^2}{\gamma_m^2 + \omega^2 k^2}\right\}$$

Define $$-\psi\delta_k c_k^{-1} \equiv W_k + iX_k$$

so that $$c_k = -\delta_k \psi \left(W_k - iX_k\right)/\left(W_k^2 + X_k^2\right)$$

and then define finally

$$w_k + ix_k \equiv c_k \left(= \left[\frac{-\delta_k \psi W_k}{W_k^2 + X_k^2}\right] + i\left[\frac{\delta_k \psi X_k}{W_k^2 + X_k^2}\right]\right)$$

Noting that $c_{-k} = w_k - ix_k$ and recalling that $\Phi = \sum_k c_k e^{ik\omega t}$:

$$\Phi = 2\sum_{k=1}^{\infty} \left\{w_k \cos k\omega t - x_k \sin k\omega t\right\}$$

In the computation performed on the IBM-650 computer, using this solution, the sum is carried to k = 19. The coefficients $w_k$ and $x_k$ are computed in 4-1/2 minutes. Thereafter, $\Phi(t)$ is computed in 25 seconds for each t.